
^{123}I -MIP-1072, a Small-Molecule Inhibitor of Prostate-Specific Membrane Antigen, Is Effective at Monitoring Tumor Response to Taxane Therapy

Shawn M. Hillier, Ashley M. Kern, Kevin P. Maresca, John C. Marquis, William C. Eckelman, John L. Joyal, and John W. Babich

Molecular Insight Pharmaceuticals, Cambridge, Massachusetts

Because traditional endpoints in oncology trials are not always applicable for metastatic prostate cancer, better ways of following response to treatment are needed. Prostate-specific membrane antigen (PSMA) is a transmembrane protein expressed in normal human prostate epithelium and is upregulated in prostate cancer. (S)-2-(3-((S)-1-carboxy-5-((4- ^{123}I -iodobenzyl)amino)pentyl)ureido)pentanedioic acid, ^{123}I -MIP-1072, targets PSMA and was evaluated for monitoring the growth of PSMA-positive LNCaP cells in vitro and as xenografts after paclitaxel therapy. **Methods:** LNCaP and 22Rv1 cells were treated with paclitaxel (0–100 nM) for 48 h, after which binding of ^{123}I -MIP-1072 was examined. Cell number was determined by MTS assay, and PSMA expression was analyzed by Western blotting. LNCaP xenograft-bearing mice were treated with paclitaxel (6.25 mg/kg) for 3.5 cycles of 5 d on and 2 d off. Tissue distribution of ^{123}I -MIP-1072 was determined on days 2 and 23 from the start of paclitaxel treatment. **Results:** Paclitaxel (10–100 nM) inhibited LNCaP and 22Rv1 cell growth after 48 h, and binding of ^{123}I -MIP-1072 was proportional to cell number. Western blot analysis verified there was no paclitaxel-dependent change in PSMA expression. Treatment of LNCaP xenografts with paclitaxel resulted in a decrease in tumor volume (–21%), compared with an increase in the untreated xenografts (+205%) by day 23. Tumor uptake of ^{123}I -MIP-1072 was proportional to changes in tumor mass: decreased by paclitaxel treatment and increased in untreated mice. **Conclusion:** Treatment of LNCaP cells or xenograft tumors with paclitaxel resulted in growth inhibition, which was detected with ^{123}I -MIP-1072. The high specificity of ^{123}I -MIP-1072 for prostate cancer may allow monitoring of tumor progression in patients before, during, and after chemotherapy.

Key Words: molecular imaging; oncology; radiopharmaceuticals; prostate cancer; prostate-specific membrane antigen

J Nucl Med 2011; 52:1087–1093

DOI: 10.2967/jnumed.110.086751

In 2010, it was estimated that 217,000 American men would be diagnosed with prostate cancer and 32,000 men

would die of the disease (1). Prostate-specific antigen (PSA) screening has become the primary tool in the detection of prostate cancer. However, elevated PSA levels are not always indicative of disease because men with conditions other than prostate cancer (i.e., benign prostatic hyperplasia and inflammation) also test positively (2). Additionally, 20%–30% of men with prostate cancer have serum PSA levels in the reference range, thus resulting in false-negative test results (3,4). Importantly, because PSA is a blood test, it provides little information about the location and extent of disease or the success of therapy on individual lesions.

^{18}F -FDG and capromab pendetide (ProstaScint; EUSA Pharma) are the only 2 molecular imaging agents currently approved for use in prostate cancer, although several other imaging probes, including $^{18}\text{F}/^{11}\text{C}$ -choline and $^{18}\text{F}/^{11}\text{C}$ -acetate, are being examined in the clinic (5). ^{18}F -FDG is an effective tool in the diagnosis of many cancers because it is readily taken up by hypermetabolic tumor cells (6–9). However, it is essentially ineffective in detecting prostate cancer because of the low glycolytic rate of the disease (10,11). Capromab pendetide is an ^{111}In -radiolabeled antibody that targets prostate-specific membrane antigen (PSMA) (12,13), a protein primarily expressed in normal prostate, brain, kidney proximal tubules, and intestinal brush border membranes. The expression of PSMA is dramatically increased in prostate cancer (14,15), including poorly differentiated, metastatic, and hormone-refractory disease (16). However, capromab pendetide binds to the intracellular domain of PSMA (17,18) and is not in widespread use because it detects mostly necrotic regions of prostate tumors and not viable cells. Thus, new agents that will more accurately diagnose, stage, and monitor therapeutic interventions are essential for improved patient outcomes.

We recently developed molecular imaging radiopharmaceuticals capable of detecting prostate cancer through the commonly used molecular imaging modality SPECT (19,20). Our lead compound, (S)-2-(3-((S)-1-carboxy-5-((4- ^{123}I -iodobenzyl)amino)pentyl)ureido)pentanedioic acid (^{123}I -MIP-1072), is currently being investigated in clinical trials for the detection of metastatic prostate cancer. ^{123}I -MIP-1072 is a small-molecule (molecular weight, 535), glutamate-

Received Dec. 16, 2010; revision accepted Mar. 21, 2011.
For correspondence or reprints contact: John W. Babich, Molecular Insight Pharmaceuticals, 160 Second St., Cambridge, MA 02142.
E-mail: jbabich@molecularinsight.com
COPYRIGHT © 2011 by the Society of Nuclear Medicine, Inc.

urea heterodimer that competitively inhibits the *N*-acetylated α -linked acidic dipeptidase (NAALADase) enzymatic activity of PSMA. In preclinical studies, ^{123}I -MIP-1072 was shown to bind specifically and with high affinity to PSMA, internalize in prostate cancer cells that express PSMA, and accumulate in human prostate cancer xenografts in vivo. ^{123}I -MIP-1072 is cleared rapidly from nontarget tissues and is primarily excreted through the urine (20). In early clinical trials, ^{123}I -MIP-1072 was shown to detect both bone and soft-tissue metastatic lesions in patients with radiologically proven prostate cancer (21).

Localized prostate cancer is often eradicated through radical prostatectomy or external-beam radiation. For metastatic disease, androgen ablation therapy provides symptomatic relief and increases life expectancy by approximately 1–2 y in most men, but the relief is temporary because patients eventually relapse into hormone-refractory prostate cancer (22,23). Taxane (paclitaxel or docetaxel) chemotherapy is one of the few therapeutic options for the treatment of hormone-refractory prostate cancer and has shown efficacy in at least half of patients (24–26). Given that these patients have the fewest options, a better understanding of their disease progression could result in improved patient outcomes—those who do not respond to taxane intervention could quickly be placed on another chemotherapeutic regimen or on an investigational drug.

Because ^{123}I -MIP-1072 was shown to be capable of detecting prostate cancer xenografts in mice, we sought to examine its ability to monitor the success or failure of chemotherapy. Here, we evaluate the ability of ^{123}I -MIP-1072 to detect changes in LNCaP and 22Rv1 (PSMA-expressing prostate cancers) cell number after paclitaxel treatment in vitro and in NCr nude mice bearing LNCaP tumors that had undergone paclitaxel therapy.

MATERIALS AND METHODS

Synthesis and Radiolabeling of MIP-1072

The synthesis of MIP-1072, (*S*)-2-(3-((*S*)-1-carboxy-5-((4-iodobenzyl)amino)pentyl)ureido)pentanedioic acid, along with the radiolabeling precursor, trimethyltin-MIP-1072, and its subsequent radiolabeling with ^{123}I were described previously (19). ^{123}I -MIP-1072 is manufactured in high radiochemical purity (>95%) and specific activity (>150 GBq/ μmol).

Cell Culture

The human prostate cancer cell lines LNCaP and 22Rv1 were obtained from the American Type Culture Collection. Cell culture supplies were from Invitrogen unless otherwise noted. Cells were maintained in RPMI 1640 medium supplemented with 10% fetal bovine serum (Hyclone), 4 mM L-glutamine, 1 mM sodium pyruvate, 10 mM *N*-(2-hydroxyethyl)piperazine-*N'*-(2-ethanesulfonic acid), D-glucose (2.5 mg/mL), and gentamicin (50 $\mu\text{g}/\text{mL}$) in a humidified incubator at 37°C/5% CO₂. Cells were removed from flasks for passage or for transfer to 24-well assay plates by incubating them with 0.25% trypsin/ethylenediaminetetraacetic acid.

Cell Binding

LNCaP and 22Rv1 cells (0.25–2 $\times 10^5$ cells per well or 1 $\times 10^5$ cells per well for paclitaxel treatment, in 24-well plates in dupli-

cate) were incubated in growth medium supplemented with 0, 1, 10, or 100 nM paclitaxel (LC Laboratories) for 48 h. Cells were then pulsed with 3 nM ^{123}I -MIP-1072 and incubated at room temperature for 1 h. Cells were gently removed from wells, washed twice with D-PBS (Dulbecco's phosphate-buffered saline, catalog no. 14190; Invitrogen) and counted in an LKB Wallac automated γ -counter (model 1282; Perkin Elmer).

Assessment of Cell Number

LNCaP and 22Rv1 cells (0.25–2 $\times 10^5$ cells per well or 1 $\times 10^5$ cells per well for paclitaxel treatment, in 24-well plates in duplicate) were incubated in growth medium supplemented with 0, 1, 10, or 100 nM paclitaxel for 48 h. At the end of the incubation period, cell number was determined using the CellTiter 96 Aqueous Non-Radioactive Cell Proliferation Assay (Promega) according to the manufacturer's instructions. Briefly, 3-(4,5-dimethylthiazol-2-yl)-5-(3-carboxymethoxyphenyl)-2-(4-sulfophenyl)-2H-tetrazolium, inner salt (MTS), and phenazine methosulfate substrates were combined as recommended and added to each well of the 24-well plate, and the absorbance was measured at 490 nm in a Victor³ Multilabel Counter (model 1420; Perkin Elmer). Relative cell number was calculated by fixing the 0 nM paclitaxel as 100%. Additionally, some cells were washed with D-PBS, trypsinized, and counted using a hemocytometer and trypan blue exclusion to determine actual cell number.

Western Blot

LNCaP and 22Rv1 cells (1 $\times 10^5$ cells per well in 24-well plates in duplicate) were incubated in growth medium supplemented with 0, 1, 10, or 100 nM paclitaxel for 48 h. The cells were washed with D-PBS and then lysed in 0.2 mL of radioimmunoprecipitation assay buffer (Cell Signaling Technology) supplemented with protease inhibitor cocktail (Sigma Aldrich). Protein concentrations were determined using the Bio-Rad DC Protein Assay Reagents at a wavelength of 750 nm. Equal amounts of total protein (20 μg) were loaded for sodium dodecyl sulfate polyacrylamide gel electrophoresis (SDS-PAGE) (NuPage; Invitrogen), transferred to polyvinylidene difluoride membrane, and probed overnight with an anti-PSMA antibody (sc-10269; Santa Cruz Biotechnology). Horseradish peroxidase-conjugated secondary antibody (Santa Cruz Biotechnology) was incubated for 1 h at room temperature. Proteins were visualized using the SuperSignal West Pico Chemiluminescent Substrate kit (Pierce) according to the manufacturer's instructions, exposed to radiographic film, and processed using a Kodak X-OMAT 1000A film processor. The Western blot signal was quantified using ImageJ software (National Institutes of Health).

Inoculation of Mice with Xenografts

All animal studies were approved by the Institutional Animal Care and Use Committee in accordance with the guidelines set forth by the U.S. Public Health Service *Policy on Humane Care and Use of Laboratory Animals* (<http://grants.nih.gov/grants/olaw/references/phspol.htm>). Mice were housed under standard conditions in approved facilities with 12-h light–dark cycles and given food and water ad libitum. Male athymic NCr-*nu/nu* mice were purchased from Taconic. Mice were anesthetized by an intraperitoneal injection of avertin (0.5 mL/mouse, 19 mg/mL). For inoculation in mice, LNCaP cells were resuspended at 10⁷ cells/mL in a 1:1 mixture of PBS with glucose (1 g/L) and sodium pyruvate (36 mg/L) (Invitrogen):Matrigel (BD Biosciences). Each mouse was injected in the right flank with 0.25 mL of the cell suspension. Mice were studied when the tumors reached approximately 400 mm³.

Paclitaxel Administration to Mice

Ethanol (497 μ L) and Cremophor-EL (527 μ L; Sigma-Aldrich.) were added to paclitaxel (6 mg), sonicated, and then diluted with 0.9% sodium chloride for a final ratio of 13.0:13.7:73.3 (ethanol:Cremophor-EL:0.9% sodium chloride). LNCaP xenograft-bearing mice were injected intraperitoneally with paclitaxel (6.25 mg/kg) or vehicle only for 3.5 cycles of 5 d on and 2 d off (21 d total). Tumors were measured with Vernier calipers 3 times per week, and tumor volume was calculated as $\pi/6(d_1)^2(d_2)$, where d_1 is the shorter diameter and d_2 is the longer diameter.

Mouse Tissue Distribution

The tissue distribution was quantitatively analyzed in separate groups of male NCr-*nu/nu* mice bearing LNCaP cell xenografts on days 2 and 23 after the administration of paclitaxel or vehicle control. ^{123}I -MIP-1072 was administered via the tail vein as a bolus injection (~ 74 kBq/mouse at a specific activity of > 150 GBq/ μ mol) in a constant volume of 0.05 mL. The animals ($n = 9$ /group) were euthanized by asphyxiation with carbon dioxide at 1 h after injection. Tissues (blood, heart, lungs, liver, spleen, kidneys, intestines [with contents], skeletal muscle, and tumor) were dissected, excised, weighed wet, and counted in an automated γ -counter. Tissue time-radioactivity levels, expressed as percentage injected dose (%ID) and %ID per gram of tissue (%ID/g), were determined.

Immunohistochemistry

LNCaP tumors were fixed in formalin for 24 h, transferred to ethanol, and processed by Mass Histology Services, Inc. Briefly,

tumors were paraffin-embedded and sectioned for Harris hematoxylin and eosin staining. Ki-67 was stained using the Dako mouse antihuman antigen (M7240 clone MIB-1) at a 1:50 dilution for 1 h at room temperature after a 20-min heat pretreatment in citrate buffer (H-3300; Vector Labs). PSMA was detected using the Dako mouse antihuman PSMA (M3620 clone 3E6¹) at a 1:75 dilution for 1 h at room temperature after a 20-min heat pretreatment in citrate buffer. The secondary antibody was biotin-labeled goat antimouse IgG, and the streptavidin was the Vectastain ABC kit with the 3,3'-diaminobenzidine (DAB) chromagen (Vector Labs). Slides were visualized and photographed using a Nikon Eclipse 80i microscope.

RESULTS

^{123}I -MIP-1072 Tracks Changes in LNCaP and 22Rv1 Cell Number

The ability of ^{123}I -MIP-1072 to track changes in LNCaP and 22Rv1 cell number was initially examined in vitro. ^{123}I -MIP-1072 binding to 0.25×10^5 , 0.5×10^5 , 1×10^5 , and 2×10^5 cells was shown to be linear with respect to cell number (Fig. 1A). Fewer total femtomoles bound to 22Rv1 cells than to LNCaP cells, likely indicating lower PSMA expression in the former cell line.

Cells were treated with 0–100 nM paclitaxel for 48 h and subsequently pulsed with ^{123}I -MIP-1072. At 10 and 100 nM paclitaxel, cell number, as determined by MTS assay, was $54.1\% \pm 2.5\%$ and $59.1\% \pm 0.8\%$ of untreated LNCaP cells,

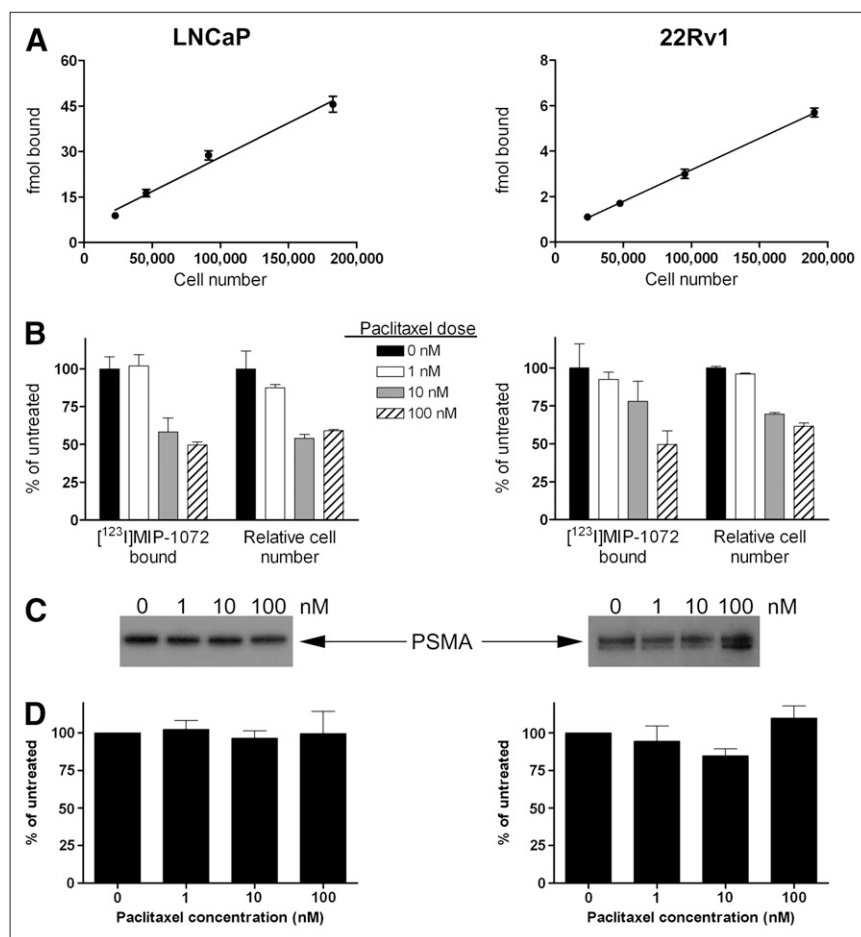


FIGURE 1. ^{123}I -MIP-1072 tracks changes in LNCaP and 22Rv1 cell number. (A) LNCaP and 22Rv1 cells (~ 0.25 – 2×10^5 cells per well) were incubated with ^{123}I -MIP-1072 for 1 h, after which femtomoles bound were determined. Actual cell number was determined by washing with PBS, trypsinizing, and counting cells with a hemocytometer. (B) LNCaP and 22Rv1 cells were treated with 0–100 nM paclitaxel for 48 h and then pulsed with ^{123}I -MIP-1072 for 1 h. Cell number was determined by MTS assay. (C) Western blot analysis of LNCaP and 22Rv1 cells treated with 0–100 nM paclitaxel for 48 h. Equal amount of protein was loaded onto each well of SDS-PAGE gel and probed for PSMA expression. (D) Quantitative densitometry of Western blots. PSMA protein expression from 3 LNCaP and 2 22Rv1 Western blots was quantified using ImageJ software. Data are expressed as percentage of 0 nM paclitaxel.

respectively, and $69.7\% \pm 0.8\%$ and $61.5\% \pm 2.3\%$ of untreated 22Rv1 cells, respectively (Fig. 1B). Similarly, at these concentrations of paclitaxel, the binding of ^{123}I -MIP-1072 was approximately 40%–50% lower than that of the untreated LNCaP or 22Rv1 cells (Fig. 1B). The diminished binding was found to be directly proportional to the decrease in relative cell number at these doses of paclitaxel.

To confirm that the reduced binding of ^{123}I -MIP-1072 was indeed due to paclitaxel-mediated growth inhibition and not a result of cell death, LNCaP cells were plated at 4×10^5 cells per well in 6-well plates and treated with or without 100 nM paclitaxel. After 48 h, there were still 4.6×10^5 cells per well in the paclitaxel-treated group, whereas the cell number increased to 1.3×10^6 cells per well in the untreated wells. Trypan blue exclusion demonstrated that both the treated and untreated cells were more than 95% viable.

To verify that the reduced binding of ^{123}I -MIP-1072 was not a result of decreased expression of PSMA, Western blotting was conducted. Equal amounts of LNCaP and 22Rv1 cellular lysate were loaded for SDS-PAGE. Representative blots are depicted in Figure 1C. The intensity of the PSMA signal on the Western blot was 10-fold less with 22Rv1 cells, explaining the lower binding of ^{123}I -MIP-1072 in Figure 1A. Quantitative densitometry was conducted to determine whether PSMA expression per cell was altered by paclitaxel treatment. Figure 1D depicts the results of independent measurements from 3 LNCaP and 2 22Rv1 Western blots using ImageJ software. The analysis demonstrated that there were no significant differences in the PSMA expression in any of the paclitaxel doses.

Paclitaxel Inhibits Proliferation of LNCaP Tumors

NCr-*nu/nu* mice bearing LNCaP xenograft tumors were treated with paclitaxel (6.25 mg/kg) to inhibit tumor growth. The mice were monitored for 23 d and compared with mice receiving vehicle only. Figure 2 depicts the growth rate of both groups and shows a 205% increase over the initial volume of the vehicle-treated tumors on day 23, compared with a 21% regression in the paclitaxel treated tumors on day 23. On day 23, the tumor volume of the vehicle-treated group was 2.8-fold greater than that of the paclitaxel-treated group ($P < 0.03$).

After treatment with paclitaxel, 4 random tumors from each group were excised, formalin-fixed, and processed for markers of proliferation (Ki-67 staining) as well as PSMA expression. Ki-67 staining was highly positive in the vehicle-treated tumors, whereas the paclitaxel-treated tumors showed only minor staining (Fig. 3, representative example), confirming the growth-inhibiting activity of paclitaxel. Both vehicle- and paclitaxel-treated mice showed highly positive staining for PSMA, further documenting that PSMA expression is unchanged in LNCaP tumors treated with paclitaxel.

^{123}I -MIP-1072 Monitors Changes in Tumor Size in Response to Therapy

It is critical for an effective prostate cancer imaging agent, such as ^{123}I -MIP-1072, to be able to monitor changes in tumor size as they regress in response to therapeutic inter-

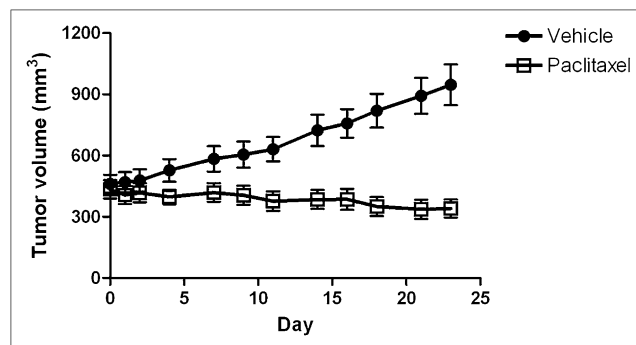


FIGURE 2. Growth of LNCaP tumors treated with paclitaxel (6.25 mg/kg) or vehicle only for 3.5 cycles of 5 d on and 2 d off. Tumors were measured 3 times per week with Vernier calipers. Data are expressed as tumor volume (mm^3).

ventions or continue to grow when they do not respond to treatment. ^{123}I -MIP-1072, in mice bearing LNCaP xenograft tumors, demonstrates a linear correlation ($R^2 = 0.7605$) between tumor mass and the %ID of ^{123}I -MIP-1072 in the tumor, as depicted in Figure 4.

On the basis of these data, we examined the ability of ^{123}I -MIP-1072 to track changes in LNCaP tumor mass after treatment with paclitaxel (6.25 mg/kg). The tissue distribution of ^{123}I -MIP-1072 after 2 d or 23 d administration of paclitaxel or vehicle only was assessed, and the results expressed as %ID/g are illustrated in Table 1. As anticipated, ^{123}I -MIP-1072 uptake was greatest in the kidney (147 ± 5 %ID/g, 156 ± 6 %ID/g, and 141 ± 6 %ID/g in the day 2 vehicle, day 23 vehicle, and day 23 paclitaxel groups, respectively), which has been shown to express high levels of NAALADase (7), and in PSMA-positive LNCaP xenografts (10.0 ± 0.6 %ID/g, 9.8 ± 0.67 %ID/g, and 13.3 ± 1.8 %ID/g in the day 2 vehicle, day 23 vehicle, and day 23 paclitaxel groups, respectively). Uptake in nontarget tissues was generally low and similar to previously reported results (20).

On a per-organ (total tissue) basis (Table 2; Fig. 5A), uptake in the tumors increased from 2.17 ± 0.29 %ID to 3.93 ± 0.49 %ID from day 2 to day 23, corresponding to an increase in tumor growth ($P < 0.01$). There was no significant difference in uptake between the day 2 vehicle group and day 23 paclitaxel group (2.17 ± 0.29 %ID to 2.34 ± 0.60 %ID, $P = 0.8$), consistent with the inhibition of tumor growth over the time period studied. There were no significant differences in kidney uptake, suggesting paclitaxel does not alter PSMA expression in the kidneys.

Figure 5A depicts the mean tumor mass and uptake of ^{123}I -MIP-1072 for each group, expressed as %ID, and Figure 5B illustrates the mass of individual tumors and their respective uptake. Tumor mass in the day 2 vehicle group ranged from 54 to 501 mg (mean, 222 ± 28 mg). As expected, tumors in the day 23 vehicle group generally exhibited a larger mass (ranging from 134 to 890 mg [mean, 415 ± 52 mg]) than did the day 2 vehicle group ($P < 0.005$) and the day 23 paclitaxel group ($P < 0.01$). After paclitaxel treatment, tumors generally exhibited a reduced

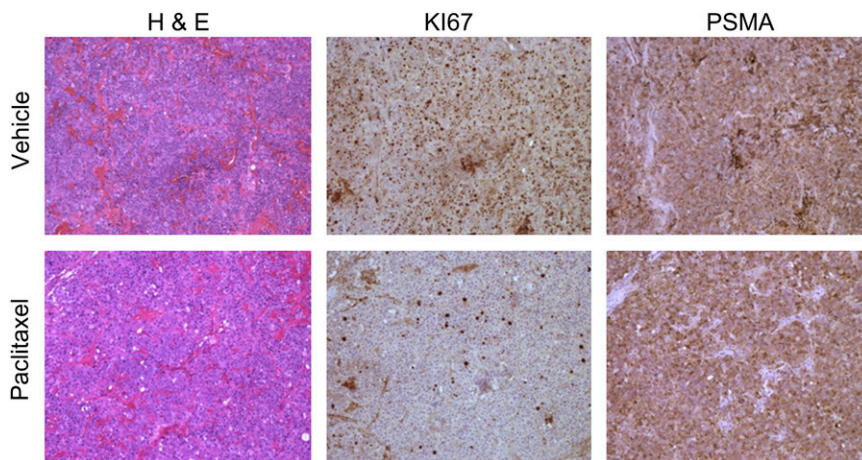


FIGURE 3. Immunohistochemical analysis of LNCaP tumors after treatment with paclitaxel (6.25 mg/kg) or vehicle for 3.5 cycles of 5 d on and 2 d off. Tumors were excised, formalin-fixed, and stained with hematoxylin and eosin (H & E), Ki-67 (proliferation marker), and PSMA.

mass, ranging from 6 to 288 mg (mean, 161 ± 46 mg); however, this mass reduction was not statistically significant as compared with the day 2 vehicle group ($P = 0.59$). One 843 mg tumor did not respond to the paclitaxel treatment but was still included in the analysis. Tumor uptake of ^{123}I -MIP-1072 was proportional to the changes in tumor mass ($R^2 = 0.7066$, Fig. 5B), decreasing in the paclitaxel treatment group and increasing in the control (vehicle) group, indicating that ^{123}I -MIP-1072 can indeed track changes in tumor size in response to therapeutic interventions.

DISCUSSION

Monitoring metastatic prostate cancer disease progression and the success of interventions remains challenging. Detection of lymph node metastases with CT and MRI is confounded by low specificity, because these modalities rely on enlarged or irregular anatomic features, frequently leading to false-negative results. Bone metastases, which are also common in prostate cancer, are monitored with radionuclide bone scans; however, because this type of scanning

detects tissue remodeling as opposed to tumor burden, false-positives are common as a result of inflammation, previous bone injuries, and arthritis. Therefore, the need exists for better methods of monitoring disease and its response to therapeutic interventions so that patients may receive the most appropriate care (27).

^{123}I -MIP-1072 was developed as a SPECT agent for diagnosing, staging, and monitoring prostate cancer. It binds to the prostate cancer-specific marker, PSMA, with high affinity and specificity, and localizes to PSMA-avid tissues in vivo (19,20). In early clinical trials in patients with radiologically confirmed metastatic prostate cancer, ^{123}I -MIP-1072 has yielded high-quality images of soft-tissue, lymph node, and bone lesions as rapidly as 1 h after injection (21). These high-quality images with ^{123}I -MIP-1072 are in contrast to images with capromab pendetide, which, as a result of prolonged blood-pool activity, requires imaging at 3–5 d after injection (12,13). In addition, partly because of poor tissue penetrability, capromab pendetide is not approved by the Food and Drug Administration for imaging bone metastases. Thus, we sought to test in preclinical models whether ^{123}I -MIP-

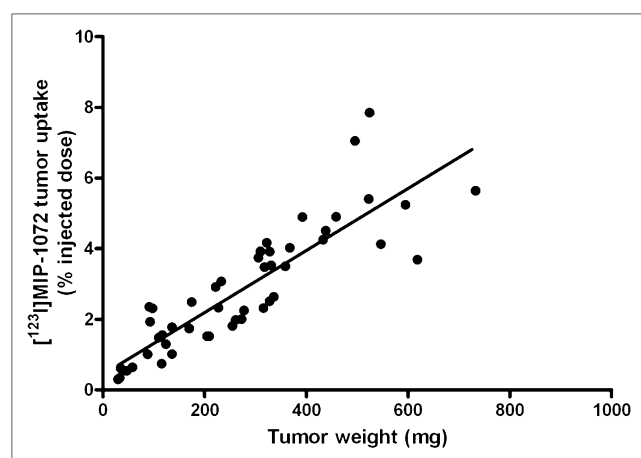


FIGURE 4. LNCaP tumor uptake of ^{123}I -MIP-1072 in untreated mice. Mice were administered ^{123}I -MIP-1072 intravenously and sacrificed after 1 h. Tumors were excised, weighed wet, and counted in an automated γ -counter. Data are expressed as %ID.

TABLE 1
Tissue Distribution of ^{123}I -MIP-1072 in NCr *nu/nu* Mice Bearing LNCaP Xenografts (%ID/g)

Tissue	Day 2		Day 23	
	Vehicle	Vehicle	Vehicle	Paclitaxel
Blood	0.81 ± 0.05	0.8 ± 0.04	0.8 ± 0.06	0.8 ± 0.06
Heart	0.55 ± 0.04	0.61 ± 0.05	0.57 ± 0.06	0.57 ± 0.06
Lungs	1.5 ± 0.09	1.56 ± 0.09	1.54 ± 0.11	1.54 ± 0.11
Liver	2.4 ± 0.09	2.45 ± 0.1	2.64 ± 0.21	2.64 ± 0.21
Spleen	3.9 ± 0.31	4.14 ± 0.43	4.85 ± 0.73	4.85 ± 0.73
Kidneys	147 ± 5	156 ± 6	141 ± 6	141 ± 6
Intestine	0.54 ± 0.03	$0.64 \pm 0.03^*$	0.54 ± 0.03	0.54 ± 0.03
Skeletal muscle	0.43 ± 0.07	0.32 ± 0.02	0.36 ± 0.05	0.36 ± 0.05
Tumor	10 ± 0.6	9.8 ± 0.67	13.3 ± 1.8	13.3 ± 1.8

* $P < 0.05$.

Data are %ID/g, expressed as mean \pm SEM.

TABLE 2
Tissue Distribution of ^{123}I -MIP-1072 in NCr *nu/nu* Mice Bearing LNCaP Xenografts (%ID)

Tissue	Day 2		Day 23	
	Vehicle	Vehicle	Vehicle	Paclitaxel
Blood	1.43 ± 0.06	1.38 ± 0.07	1.39 ± 0.08	
Heart	0.08 ± 0.01	0.08 ± 0.01	0.08 ± 0.01	
Lungs	0.29 ± 0.02	0.31 ± 0.02	0.3 ± 0.02	
Liver	3.23 ± 0.13	3.38 ± 0.13	3.81 ± 0.22*	
Spleen	0.28 ± 0.02	0.29 ± 0.03	0.3 ± 0.04	
Kidneys	66 ± 2	69 ± 1	66 ± 1	
Intestine	1.28 ± 0.06*	1.81 ± 0.08	1.74 ± 0.07	
Skeletal muscle	4.83 ± 0.66	3.55 ± 0.23	4.02 ± 0.47	
Tumor	2.17 ± 0.29	3.93 ± 0.49*	2.34 ± 0.6	

* $P < 0.05$.

Data are %ID/g, expressed as mean ± SEM.

1072 is capable of monitoring changes in disease progression or regression in response to chemotherapy both in vitro and in vivo, so that this benefit may be translated to the clinic.

Metastatic or recurrent prostate cancer in patients who have become refractory to hormonal therapy is often treated by taxane chemotherapy, which improves symptoms and survival. However, approximately 50% of patients do not respond to taxanes and are exposed to significant toxicity without direct benefit (24–26). Hence, we chose to use paclitaxel chemotherapy in our assessment of ^{123}I -MIP-1072 to determine whether it can monitor the progression or regression of disease with external imaging. Several reports have shown growth inhibition of LNCaP xenografts by paclitaxel (28,29). Consistent with these reports, we demonstrated a 40%–50% inhibition of LNCaP and 22Rv1 cell growth in culture after 48 h and a 22% growth reduction of LNCaP xenografts by paclitaxel. Importantly, ^{123}I -MIP-1072 was able to track cell number in vitro and tumor regression and progression in vivo. The results clearly show a linear relationship between tumor size and ^{123}I -MIP-1072 uptake, confirming that ^{123}I -MIP-1072 should be useful to monitor changes in tumor burden in response to therapy in a clinical setting. Similarly, because PSMA expression is maintained, and perhaps even increased, in cells in which androgens were removed (30), or in patients after androgen deprivation therapy (31), ^{123}I -MIP-1072 should also be effective in monitoring this patient population.

Western blot analysis in vitro and immunohistochemistry in vivo demonstrate that the reduced uptake of ^{123}I -MIP-1072 was not an artifact of changes in PSMA expression per cell but rather directly related to a change in tumor cell number or mass supporting the use of ^{123}I -MIP-1072 for monitoring tumor response. Several reports have indicated that PSMA expression, as opposed to other prostate-specific markers, is unchanged after taxane therapy in humans (32,33). For example, Kuroda et al. found that androgen receptor and PSA levels were downregulated in a dose-dependent

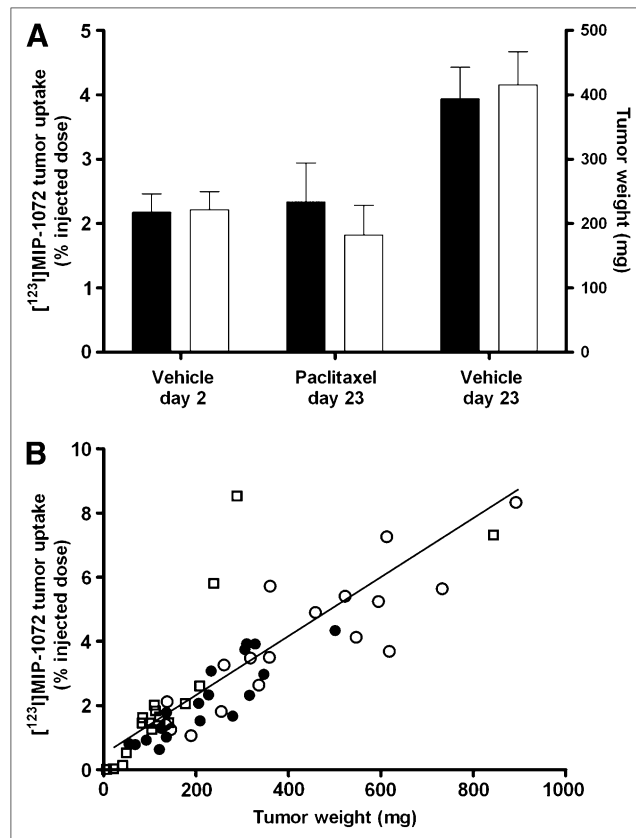


FIGURE 5. LNCaP tumor uptake of ^{123}I -MIP-1072 in paclitaxel- or vehicle-treated mice. Mice were treated with paclitaxel (6.25 mg/kg) or vehicle for 3.5 cycles of 5 d on and 2 d off. Mice were administered ^{123}I -MIP-1072 intravenously and sacrificed after 1 h. Tumors were excised, weighed wet, and counted in an automated γ -counter. (A) Uptake of ^{123}I -MIP-1072 expressed as %ID (black bars) and tumor mass (white bars) at time of sacrifice in each of 3 groups. Results are mean ± SEM. (B) Uptake of ^{123}I -MIP-1072 expressed as %ID as function of tumor mass for individual mice on day 2 (vehicle, ●) and day 23 (vehicle, ○; paclitaxel, □).

manner in response to docetaxel (33), possibly accounting for the higher PSA response rates (45%–50%) relative to the measurable response rates (8%–17%) in the 2 phase III trials that led the Food and Drug Administration to approve docetaxel in the treatment of prostate cancer (25,26). These findings further suggest that a molecular imaging radiopharmaceutical targeting PSMA would provide a better gauge of therapeutic responses than monitoring patient response through serum PSA levels or other suboptimal imaging modalities.

CONCLUSION

New imaging modalities for the diagnosis, staging, and monitoring of patient response to therapies are needed to better manage patient care and to improve long-term outcomes. The data here clearly demonstrate that ^{123}I -MIP-1072 tumor uptake is directly proportional to tumor mass and therefore can track changes in response to therapy and thus may satisfy this critical unmet need for prostate cancer. ^{123}I -MIP-1072 continues to be studied in the clinical setting to investigate

its utility for the detection of prostate cancer and distant metastases and, in the future, its ability to monitor the success of therapeutic interventions.

DISCLOSURE STATEMENT

The costs of publication of this article were defrayed in part by the payment of page charges. Therefore, and solely to indicate this fact, this article is hereby marked “advertisement” in accordance with 18 USC section 1734.

ACKNOWLEDGMENTS

This study was supported in part by the National Institutes of Health (R43 EB004253-01). This work was conducted at Molecular Insight Pharmaceuticals, Inc. No other potential conflict of interest relevant to this article was reported.

REFERENCES

1. American Cancer Society. *Cancer Facts and Figures 2010*. Available at: www.cancer.org/Research/CancerFactsFigures. Accessed May 16, 2011.
2. Tricoli JV, Schoenfeldt M, Conley BA. Detection of prostate cancer and predicting progression: current and future diagnostic markers. *Clin Cancer Res*. 2004;10:3943–3953.
3. Thompson IM, Pauler DK, Goodman PJ, et al. Prevalence of prostate cancer among men with a prostate-specific antigen level < or = 4.0 ng per milliliter. *N Engl J Med*. 2004;350:2239–2246.
4. Catalona WJ, Smith DS, Ratliff TL, et al. Measurement of prostate-specific antigen in serum as a screening test for prostate cancer. *N Engl J Med*. 1991;324:1156–1161.
5. Jadvar H. Molecular imaging of prostate cancer: a concise synopsis. *Mol Imaging*. 2009;8:56–64.
6. Yamamoto T, Seino Y, Fukumoto H, et al. Over-expression of facilitative glucose transporter genes in human cancer. *Biochem Biophys Res Commun*. 1990;170:223–230.
7. Delbeke D. Oncological applications of FDG PET imaging. *J Nucl Med*. 1999;40:1706–1715.
8. Higashi K, Ueda Y, Yagishita M, et al. FDG PET measurement of the proliferative potential of non-small cell lung cancer. *J Nucl Med*. 2000;41:85–92.
9. Reske SN, Grillenberg KG, Glatting G, et al. Overexpression of glucose transporter 1 and increased FDG uptake in pancreatic carcinoma. *J Nucl Med*. 1997;38:1344–1348.
10. Hain SF, Maisey MN. Positron emission tomography in urological tumours. *BJU Int*. 2003;92:159–164.
11. Shvarts O, Han KR, Seltzer M, et al. Positron emission tomography in urological cancer. *Cancer Control*. 2002;9:335–342.
12. Kahn D, Williams RD, Seldin DW, et al. Radioimmunoscinigraphy with ¹¹¹indium labeled CYT-356 for the detection of occult prostate cancer recurrence. *J Urol*. 1994;152:1490–1495.
13. Petronis JD, Regan F, Seldin DW. Indium-111 capromab pendetide (ProstaScint) imaging to detect recurrent and metastatic prostate cancer. *Clin Nucl Med*. 1998;23:672–677.
14. Israeli RS, Powell CT, Fair WR, Heston WD. Molecular cloning of a complementary DNA encoding prostate-specific membrane antigen. *Cancer Res*. 1993;53:227–230.
15. Horoszewicz JS, Kawinski E, Murphy GP. Monoclonal antibodies to a new antigenic marker in epithelial prostatic cells and serum of prostatic cancer patients. *Anticancer Res*. 1987;7:927–936.
16. Silver DA, Pellicer I, Fair WR, et al. Prostate-specific membrane antigen expression in normal and malignant human tissues. *Clin Cancer Res*. 1997;3:81–85.
17. Troyer JK, Beckett ML, Wright GL. Location of prostate-specific membrane antigen in the LNCaP prostate carcinoma cell line. *Prostate*. 1997;30:232–242.
18. Troyer JK, Feng Q, Beckett ML, Wright GL. Biochemical characterization and mapping of the 7E11-C5.3 epitope of the prostate-specific membrane antigen. *Urol Oncol*. 1995;1:29–37.
19. Maresca KP, Hillier SM, Femia FJ, et al. A series of halogenated heterodimeric inhibitors of prostate-specific membrane antigen (PSMA) as radiolabeled probes for targeting prostate cancer. *J Med Chem*. 2009;52:347–357.
20. Hillier SM, Maresca KP, Femia FJ, et al. Preclinical evaluation of novel glutamate-urea-lysine analogues that target prostate-specific membrane antigen as molecular imaging pharmaceuticals for prostate cancer. *Cancer Res*. 2009;69:6932–6940.
21. Barrett JA, LaFrance N, Coleman R, et al. Targeting metastatic prostate cancer [PCa] in patients with ¹²³I-MIP1072 and ¹²³I-MIP1095 [abstract]. *J Nucl Med*. 2009;50(suppl):522P.
22. Grossmann ME, Huang H, Tindall DJ. Androgen receptor signaling in androgen-refractory prostate cancer. *J Natl Cancer Inst*. 2001;93:1687–1697.
23. Debes JD, Tindall DJ. Mechanisms of androgen-refractory prostate cancer. *N Engl J Med*. 2004;351:1488–1490.
24. Smith DC, Pienta KJ. Paclitaxel in the treatment of hormone-refractory prostate cancer. *Semin Oncol*. 1999;26:109–111.
25. Tannock IF, deWit R, Berry WR, et al. Docetaxel plus prednisone or mitoxantrone plus prednisone for advanced prostate cancer. *N Engl J Med*. 2004;351:1502–1512.
26. Petrylak DP, Tangen CM, Hussain MH, et al. Docetaxel and estramustine compared with mitoxantrone and prednisone for advanced refractory prostate cancer. *N Engl J Med*. 2004;351:1513–1520.
27. Kelloff GJ, Sullivan DC, Baker H, et al. Workshop on imaging science development for cancer prevention and preemption. *Cancer Biomark*. 2007;3:1–33.
28. Agus DB, Scher HI, Higgins B, et al. Response of prostate cancer to anti-Her-2/neu antibody in androgen-dependent and -independent human xenograft models. *Cancer Res*. 1999;59:4761–4764.
29. Zheng X, Chang RL, Cui XX, et al. Effects of 12-*O*-tetradecanoylphorbol-13-acetate (TPA) in combination with paclitaxel (Taxol) on prostate cancer LNCaP cells cultured in vitro or grown as xenograft tumors in immunodeficient mice. *Clin Cancer Res*. 2006;12:3444–3451.
30. Israeli RS, Powell CT, Corr JG, et al. Expression of the prostate-specific membrane antigen. *Cancer Res*. 1994;54:1807–1811.
31. Wright GL, Grob BM, Grossman K, et al. Upregulation of prostate-specific membrane antigen after androgen-deprivation therapy. *Urology*. 1996;48:326–334.
32. Tsui P, Rubenstein M, Guinan P. Correlation between PSMA and VEGF expression as markers for LNCaP tumor angiogenesis. *J Biomed Biotechnol*. 2005;2005:287–290.
33. Kuroda K, Liu H, Kim S, et al. Docetaxel down-regulates the expression of androgen receptor and prostate-specific antigen but not prostate-specific membrane antigen in prostate cancer cell lines: implications for PSA surrogacy. *Prostate*. 2009;69:1579–1585.